SEDIMENTOLOGY the journal of the International Association of Sedimentologists

Sedimentology (2021) **68**, 737–754 doi: 10.1111/sed.12801

On the origin and significance of composite particles in mudstones: Examples from the Cenomanian Dunvegan Formation

ZHIYANG LI*† , JUERGEN SCHIEBER* and PER KENT PEDERSEN‡
*Department of Earth and Atmospheric Sciences, Indiana University, Bloomington, IN 47405, USA (E-mail: zli20@alaska.edu)
†Department of Geological Sciences, University of Alaska, Anchorage, AK 99508, USA
‡Department of Geoscience, University of Calgary, Calgary, AB, T2N 1N4, Canada

Associate Editor – Christopher Fielding

ABSTRACT

Despite the fact that mud-dominated composite particles have increasingly been recognized as important components of marine mudstones, the characteristics, types and origins of these composite particles remain poorly understood. This incomplete understanding of critical mudstone parameters (for example, depositional grain size, composition at the particle scale and provenance) severely limits the ability to accurately interpret the conditions (for example, depositional environment and climate) under which these rocks were deposited. Herein, detailed petrographic analysis was conducted in core samples from a transect of contemporaneous proximal to distal deposits from the Cenomanian Dunvegan Formation, a fluvial-dominated delta system in the Western Canada Sedimentary Basin. Within the well-developed depositional framework, mud-dominated composite particles can be tracked along the depositional profile of the Dunvegan Formation from the fluvial to the marine realm (from incised valley to distal prodelta). By following these particles from source (hinterland erosion) to sink (offshore deposition), the origin and dispersal of various types of mud-dominated composite particles in marine mudstones can be unequivocally determined. Mud-dominated composite particles derived from a wide range of origins are differentiated. Allochthonous mud-dominated composite particles, supplied by rivers draining the hinterland, comprise volcanic rock fragments (vitric or felsic in composition), chert fragments, shale lithics (clay-mineral-rich or quartz-rich in composition), metamorphic rock fragments and chlorite/siderite clasts. Autochthonous mud-dominated composite particles include rip-up clasts (argillaceous, siderite or siliceous in composition) formed from intra-basinal erosion and contemporaneous floccules. The recognition of mud-dominated composite particles shows that the Dunvegan prodelta 'mudstones' are much coarser grained and more heterogeneous in terms of their petrographic composition than the grain size of their component minerals would suggest. Results of this study call for a critical reappraisal of the composition and actual grain size of mudstones in general. Recognition of mud-dominated composite particles can provide valuable insights to unravel their provenance, transport history and depositional setting, and will greatly enhance their utility as palaeoenvironmental archives.

Keywords Dunvegan Formation, floccule, lithic fragment, mudstone, petrography, rip-up clast.

INTRODUCTION

Mudstones are fine-grained sedimentary rocks composed dominantly of clay-sized (<4 μm) and silt-sized (4.0 to 62.5 μm) grains (Lazar *et al.*, 2015), and have been widely used to infer changes in climate and environmental conditions through geological time (Sageman *et al.*, 2003; Potter *et al.*, 2005; Macquaker & Bohacs, 2007). Their suitability for this purpose is predicated on the assumption that their apparent homogeneity relates to relatively simple provenance (for example, products of chemical weathering) and transport history. Recent petrographic studies of some marine mudstones, however, have revealed that these rocks may consist of common coarse silt to sand-sized mud-dominated composite particles (MCPs) (particles consisting of multiple clay-sized or silt-sized mineral grains; *sensu* Li & Schieber, 2018). If the depositional grain size of mudstones can be determined to be relatively coarse due to the dominant presence of MCPs (rather than fine-grained based on the apparent grain size after compaction), the transport and deposition of muds are likely subject to more complex and dynamic processes (for example, traction currents) besides passive settling from suspension (Plint, 2014; Schieber, 2016; Laycock *et al.*, 2017; Schieber *et al.*, 2019).

Notwithstanding the importance of MCPs for understanding the depositional processes of mudstones, their origins are not easily ascertained. Without careful SEM (scanning electron microscopy) imaging of high quality polished surfaces (for example, ultra-thin thin sections and ion-milled samples), it can be very challenging to unambiguously differentiate among various types of MCPs as well as identify them as discrete entities within the enclosing fine-grained matrix. Moreover, without an understanding of the distribution of different types of MCPs across different depositional environments, the origin of MCPs in mudstones cannot be comprehensively appreciated, limiting the ability to accurately decipher the climatic and environmental signals contained in these sediments.

This study focuses on the allomember E1 of the Dunvegan Formation, an ancient fluvial-dominated delta system. Although MCPs have been previously documented as a volumetrically significant component in the Dunvegan prodelta mudstones (Plint, 2014), the dispersal of MCPs along the depositional profile was not critically examined, leading to questions as to whether the observed MCPs are of autochthonous (Plint, 2014; Plint & Cheadle, 2015) or allochthonous (Schieber, 2015) origin. The well-developed depositional and stratigraphic framework of the Dunvegan Formation (Bhattacharya & Walker, 1991a,b) provides a unique opportunity to track MCPs from source (hinterland erosion) to sink (offshore deposition). In this study, coeval deposits from the proximal trunk river to distal prodelta/offshore environments were first traced and sampled based on subsurface correlations and then examined through detailed petrographic analysis, allowing for a much enhanced understanding of the origin and dispersal of various types of MCPs in marine mudstones. The characteristics, distribution and abundance of MCPs present in these strata, are summarized below.

GEOLOGICAL SETTING

The early to mid-Cenomanian Dunvegan Formation represents a large fluvial-dominated delta complex deposited into the north-western part of the Cretaceous Western Interior Seaway (Plint & Wadsworth, 2003). The seaway was situated within a broad foreland basin that had formed in response to flexural loading by the Sevier thrust belt to the west (Kauffman, 1985). The depositional and allostratigraphic framework of the Dunvegan Formation is described in detail by Bhattacharya & Walker (1991a,b). Within the Dunvegan Formation, seven allomembers have been correlated and mapped based on regional transgressive surfaces (Fig. 1). The focus of this study, allomember E1, was deposited during a lowstand of sea level. It consists of an extensive tributary incised-valley system and a trunk valley in the north-west that directly feeds river-dominated delta front and prodelta deposits towards the south-east (Fig. 1; Plint & Wadsworth, 2003).

METHODS

The facies scheme developed for the Dunvegan Formation by Bhattacharya & Walker (1991a) is adopted here. A total of 19 samples including the incised channel fill, river-dominated delta front (distributary channel or mouth bar) and prodelta facies associations of allomember E1

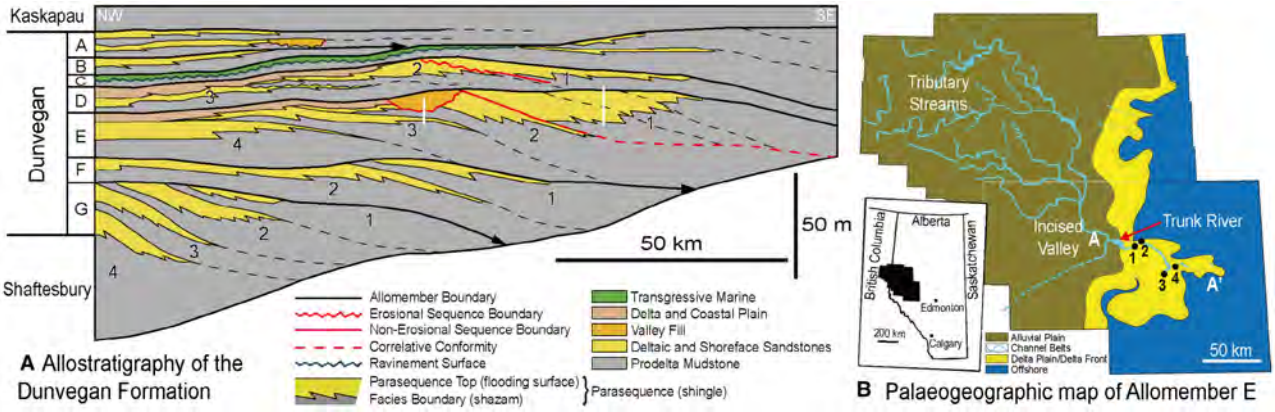

Fig. 1. (A) Regional cross-section across the Western Canada Sedimentary Basin illustrating the allostratigraphic interpretation of the Dunvegan Formation (from Bhattacharya & Walker, 1991a,b). The Dunvegan Formation comprises several stacked allomembers ('G' to 'A'), each of which consists of several smaller-scale parasequences mapped as sandy delta lobes and associated prodelta mudstones. The delta lobe of allomember E1 can be correlated updip to a feeder valley. Cores located at both proximal (cores 1 and 2) and distal (cores 3 and 4) settings (white bars) were sampled. (B) Map of valleys and lowstand deltas in allomember E of the Dunvegan (Bhattacharya & MacEachern, 2009). The location of regional cross-section shown in (A) is indicated by A–A'.

were collected from four cores to make polished thin sections and ion-milled samples (Fig. 2). Both mudstones and sandstones were sampled from each facies association.

Detailed petrographic examination of polished thin sections and ion-milled samples were conducted using a petrographic microscope and a FEI Quanta 400 scanning electron microscope (SEM) (FEI, Hillsboro, OR, USA). The SEM was operated at 15 kV and a working distance of 10 mm. Energy-dispersive X-ray spectroscopy (EDS) was used to determine the composition and mineralogy of individual grains. Through integrated optical microscopy and SEM analysis, the characteristics and origin of the various types of MCPs (Table 1), as well as their distribution from proximal (incised valley) to distal (prodelta) deposits, were determined.

To quantitatively characterize the abundance and grain-size distribution of MCPs across different depositional environments, interpreted outlines of all MCPs in representative SEM photomicrographs (four to five representative views from each sample) from the incised valley to prodelta deposits were first manually traced in Adobe Illustrator©. Abundances (volume by 2D area) and grain size (circle equivalent diameter) of different types of MCPs in these same photomicrographs were then measured with the image analysis software ImageJ.

OBSERVATIONS

Types and origins of mud-dominated composite particles

Based on compositional and textural contrast with the surrounding fine-grained matrix (areas consisting dominantly of clay-sized to fine-silt-sized grains while no distinct MCPs can be identified), six general types of MCPs can be distinctly identified (Types A to F in Table 1). These include volcanic rock fragments (Fig. 3), chert fragments (Fig. 4), shale lithics (Fig. 4), metamorphic rock fragments (Fig. 5), chlorite/siderite clasts (Fig. 6) and mud rip-up clasts (Figs 7 and 8). Floccules (Type G in Table 1) are presumably another important type of MCPs present in the Dunvegan prodelta mudstones, but they cannot always be recognized directly (Fig. 7D). Detailed characteristics (composition and texture) of each type of MCP and their possible origins are summarized in Table 1. The MCPs that are relatively 'hard' (compaction-resistant) include volcanic rock fragments, chert fragments, shale lithics, metamorphic rock fragments and chlorite/siderite clasts. Relatively 'soft' MCPs, including argillaceous mud rip-up clasts and floccules, show highly 'flattened' or strongly indented/deformed shapes (Fig. 7). Mud rip-up clasts that are siliceous or sideritic in composition are more resistant to compaction (Figs 7E and 8).

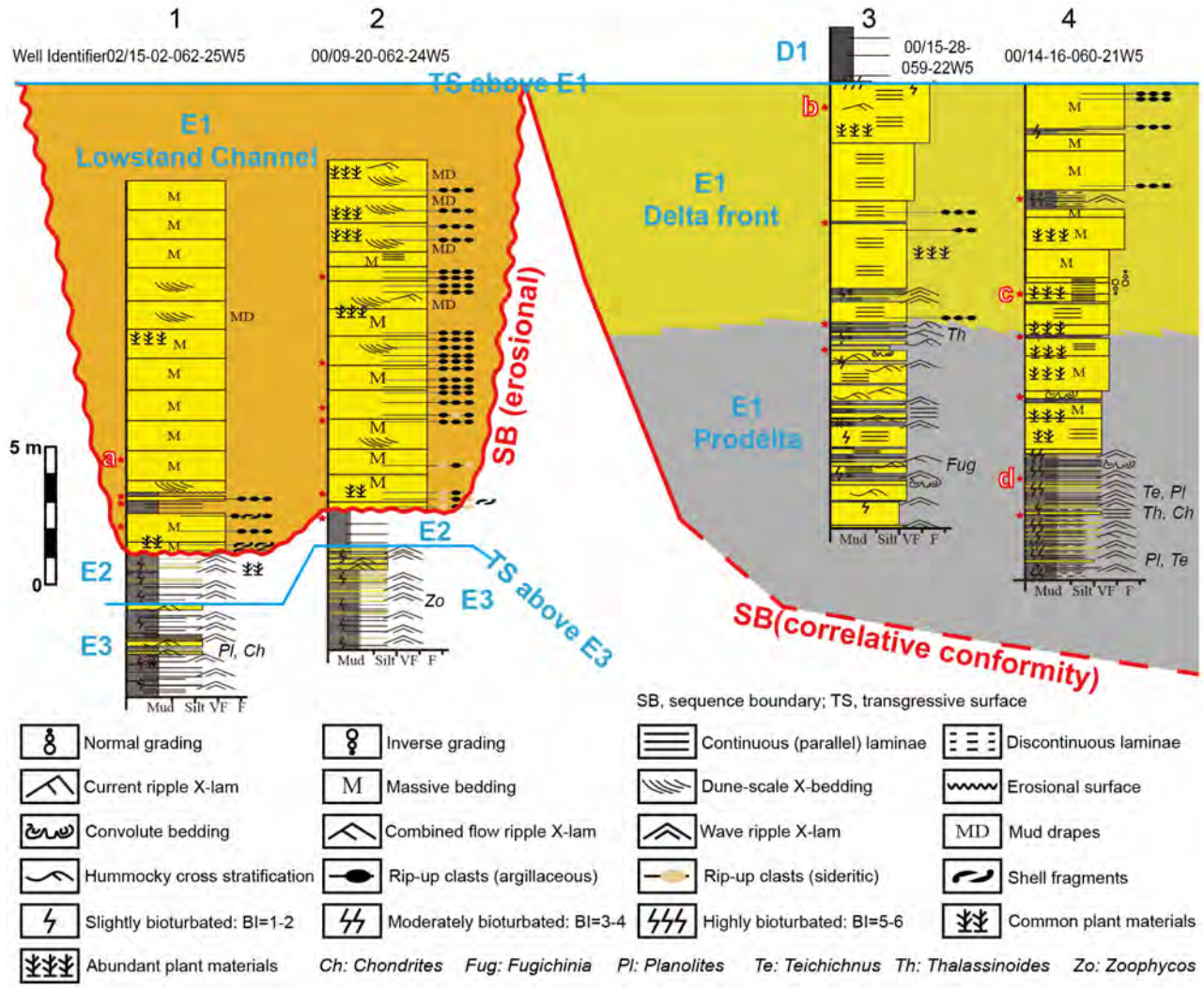

Fig. 2. Correlation of sampled cores 1 to 4 within the depositional and allostratigraphic framework shown in Fig. 1. Note the base of incised valley system of allomember E1 truncates portions of allomember E2 in the proximal setting. See Fig. 1A for legend of facies associations. Red stars represent sampling locations. Representative scanning electron microscopy (SEM) images of incised valley, proximal delta front, distal delta front and prodelta facies shown in Fig. 9 are from samples a, b, c and d, respectively.

Two subtypes of volcanic rock fragments were identified, including vitric (Type A1) and felsic (Type A2) ones. Vitric volcanic rock fragments consist of mostly illite and a small amount micrometre-sized mineral grains such as quartz, feldspar and biotite (Fig. 3A and B), similar to the mineral composition and texture of volcanic ash after burial diagenesis in marine environments (i.e. volcanic glass altered into smectite during early diagenesis, then into illite during deeper burial; Li *et al.*, 2020). The original flux of most volcanic ash into the Dunvegan system was probably wind-transported (Nadeau & Reynolds, 1981). Different from vitric volcanic rock fragments, felsic volcanic rock fragments may contain feldspar, quartz and biotite; and commonly show intergrowth texture (Fig. 3C and D). Different compositions and textures indicate different sources and transport mechanisms between the two subtypes of volcanic rock fragments. Felsic volcanic rock fragments were likely derived from rivers that drained the volcanic hinterland.

Type B (chert fragment) and Type C (shale lithics) MCPs are sedimentary rock fragments (Fig. 4). Chert fragments can be easily recognized

Table 1. Summary of petrographic characteristics of seven general types ('A' to 'G') of mud-dominated composite particles (MCPs) identified in this study.

Type of MCP	Composition	Texture	Origin
A1. Volcanic rock fragment (altered volcanic glass)	Mostly illite (volcanic glass altered into smectite during early diagenesis, then into illite during deeper burial) and a small amount micrometre-size feldspar/quartz	Usually equidimensional but can be elongated. Illite shows weakly crenulated to filamentous morphology, commonly indented by surrounding harder grains	Early diagenetic alteration products of volcanic ash (Li *et al.*, 2020). The volcanic ash was probably wind-borne initially but was also subject to reworking and transport by bottom currents
A2. Volcanic rock fragment (felsic)	Quartz, feldspar (K-spar, Na/Ca plagioclase) and biotite. Sometimes feldspars can be partially to completely altered into clays (e.g. chlorite, illite)	Intergrowth of feldspar (both plagioclase and K-spar), quartz and biotite. Compaction resistant	Derived from rivers that drained the volcanic hinterland
B. Chert fragment	Microcrystalline quartz, sometimes contains small amounts of clays	Characterized by 'salt and pepper' texture in thin sections and a very uniform appearance with scattered clay flakes under the SEM. Outlines of individual micrometre-sized quartz crystals within chert can hardly be recognized even under the SEM	Derived from erosion of older strata of chert. Could possibly be related to the chert formed in association with Precambrian iron formations, which was also possibly associated with chlorite/siderite-rich rocks (see possible origin of chlorite/siderite clast)
C1. Clay-mineral-rich shale lithic	Mostly clay minerals (dominantly illite) and varying amount (5 to 40%) of quartz (usually in the very fine to fine silt size range, sometimes show overgrowth)	Can have a uniform appearance or show preferred orientation of quartz grains and clay flakes (due to compaction). They are lithic fragments of fully compacted mudstones and thus are compaction-resistant (but can be indented by surrounding harder particles)	Derived from erosion of older strata of mudstones/shales (exposed in the hinterland) that have high clay mineral content
C2. Quartz-rich shale lithic	Dominantly quartz (fine silt to medium silt size) and a minor amount of clays	Detrital quartz silt grains can sometimes be cemented by silica. They are lithic fragments of quartz-rich mudstones (harder than clay-mineral-rich shale lithics)	Derived from erosion of older strata of quartz-rich mudstones/shales (exposed in the hinterland)
D. Metamorphic rock fragment	Quartz, illite/chlorite/mica-dominated matrix	Quartz grains are usually characterized by high aspect ratio. Illitic or micaceous minerals show preferred orientation. Some show foliated texture (e.g. foliated polycrystalline aggregates of quartz and mica)	Derived from rivers that drained the metamorphic hinterland
E. Chlorite/siderite clast	Chlorite and siderite	Siderite crystals disseminated within a 'chlorite matrix'. Siderite can be lozenge-shaped or equidimensional-shaped. Highly variable shapes, usually are indented by surrounding hard grains	Probably derived from erosion of chlorite/siderite-rich rocks associated with Precambrian iron formations exposed in the catchment area

Table 1. (continued)

Type of MCP	Composition	Texture	Origin
F1. Argillaceous rip-up clast	Mostly clay minerals (illite) and a small amount of micrometre-size quartz grains. Some contain small amounts of organic matter, pyrite or siderite	Significantly 'flattened', elongated to irregular shape, high aspect ratio, commonly strongly indented by surrounding hard grains and deformed (wrapping around rigid grains)	Derived from intra-basinal erosion/reworking of surficial or shallowly buried muds that had become sufficiently cohesive to resist disaggregation during subsequent erosion and transport
F2. Sideritic rip-up clast	Contain common scattered siderite crystals or are fully cemented by siderite. Some clasts contain small amounts of 'floating' quartz and clays	If containing <50% siderite (siderite-bearing), elongated to irregular shape (soft); with increasing amount of siderite, the clasts become harder and more resistant to compaction	Derived from reworking and erosion of siderite-rich muddy substrate or siderite nodules (early diagenetic products)
F3. Siliceous (benthic-foraminifera-like) rip-up clast	Dominantly <10 μm quartz grains (can contain larger grains) cemented by 'clean' quartz	Shapes vary, can be equidimensional or elongated, compaction-resistant. Detrital quartz grains (falls mostly within the fine-silt size category) cemented by silica	Derived from reworking of surficial or shallowly buried muds containing benthic agglutinated foraminifera (Pike & Kemp, 1996)
G. Floccule	Consists dominantly of clay minerals with admixture of fine silt and organic debris	Shows a relatively uniform texture. Although outlines of individual floccules cannot be discerned under most conditions, it is presumed that floccules constitute a significant portion of the so-called 'fine-grained matrix'	Micron size clay minerals and other small particles held together by van der Waals forces (Schieber *et al.*, 2007)

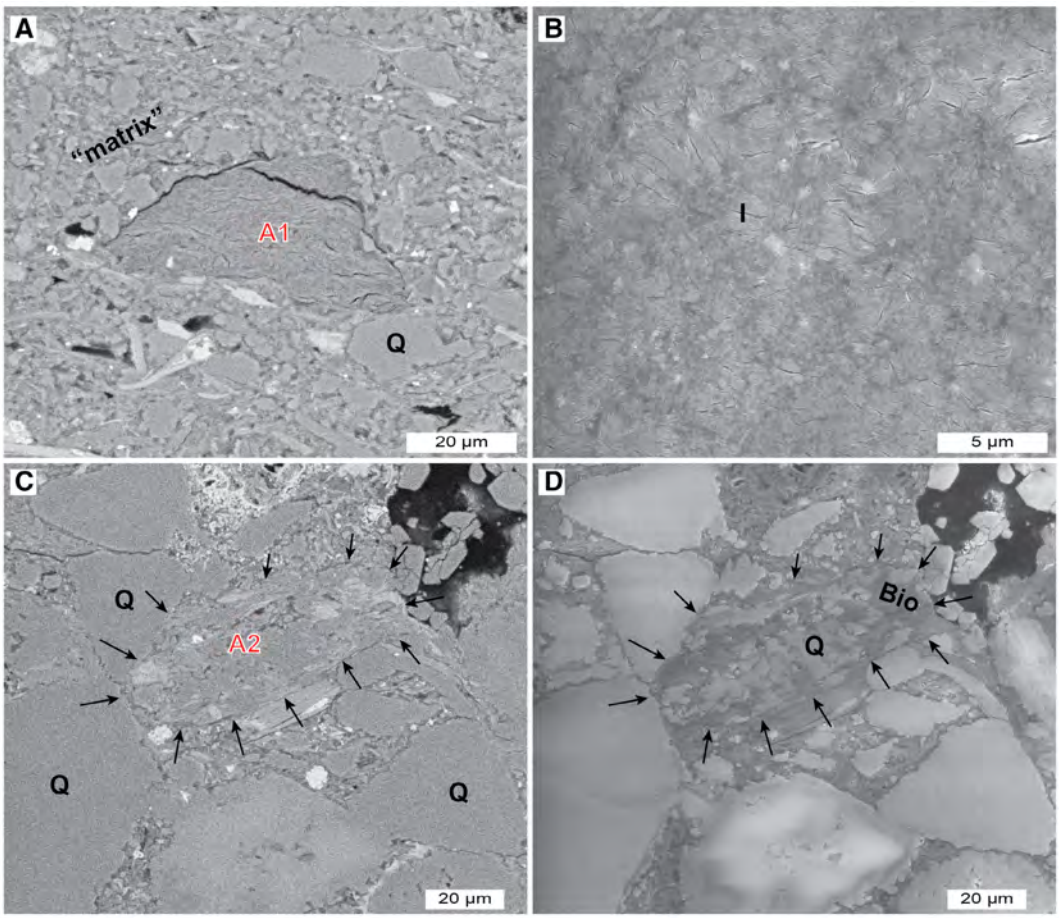

Fig. 3. Scanning electron microscopy (SEM) photomicrographs showing petrographic characteristics of volcanic rock fragments. Red letters indicate different types of mud-dominated composite particles (MCPs) as listed in Table 1. Black letters are abbreviations for different minerals. (A) A type A1 MCP (vitric volcanic rock fragment) surrounded by fine-grained matrix (consisting dominantly of clay-sized to fine-silt-sized grains) in a prodelta mudstone sample. (B) Closer view of a type A1 MCP. Vitric volcanic rock fragment consists dominantly of illite, which is recognized based on the weakly crenulated to filamentous morphology and distinct K peak suggested by energy-dispersive X-ray spectroscopy (EDS). (C) and (D) A type A2 MCP (felsic volcanic rock fragment) in a prodelta mudstone sample. Felsic volcanic rock fragments show intergrowth of quartz, feldspar and sometimes biotite. Q, quartz; I, illite; Bio, biotite. (A) and (C) are backscatter images. (B) and (D) are secondary electron images.

based on the 'salt and pepper' texture under cross-polarized light and dominant microcrystalline fabric under the SEM (Fig. 4A and B). Shale lithics show essentially the same characteristics as fully compacted mudstones/shales, and therefore are resistant to compaction and act as framework grains (Fig. 4C to F). Based on differences in composition, Type C MCPs can be subdivided into Type C1 clay-mineral-rich shale lithics (Fig. 4C and D) and Type C2 quartz-rich shale lithics (Fig. 4E and F). Both chert fragments and shale lithics were derived from recycled sedimentary rocks (i.e. older chert and mudstones/shales of different compositions).

Type D MCPs (metamorphic rock fragments) can be recognized based on the elongated quartz crystals, preferred orientation of clay minerals such as illite, chlorite and mica (Fig. 5). Some metamorphic rock fragments show foliated texture. Metamorphic rock fragments were likely derived from rivers that drained the metamorphic hinterland.

Type E MCPs (chlorite/siderite clasts) consist of siderite and chlorite (Fig. 6). Shapes of chlorite/siderite clasts are highly variable, largely due to indentation by surrounding harder grains (Fig. 6A). Based on the high iron content, these clasts were probably derived from erosion of

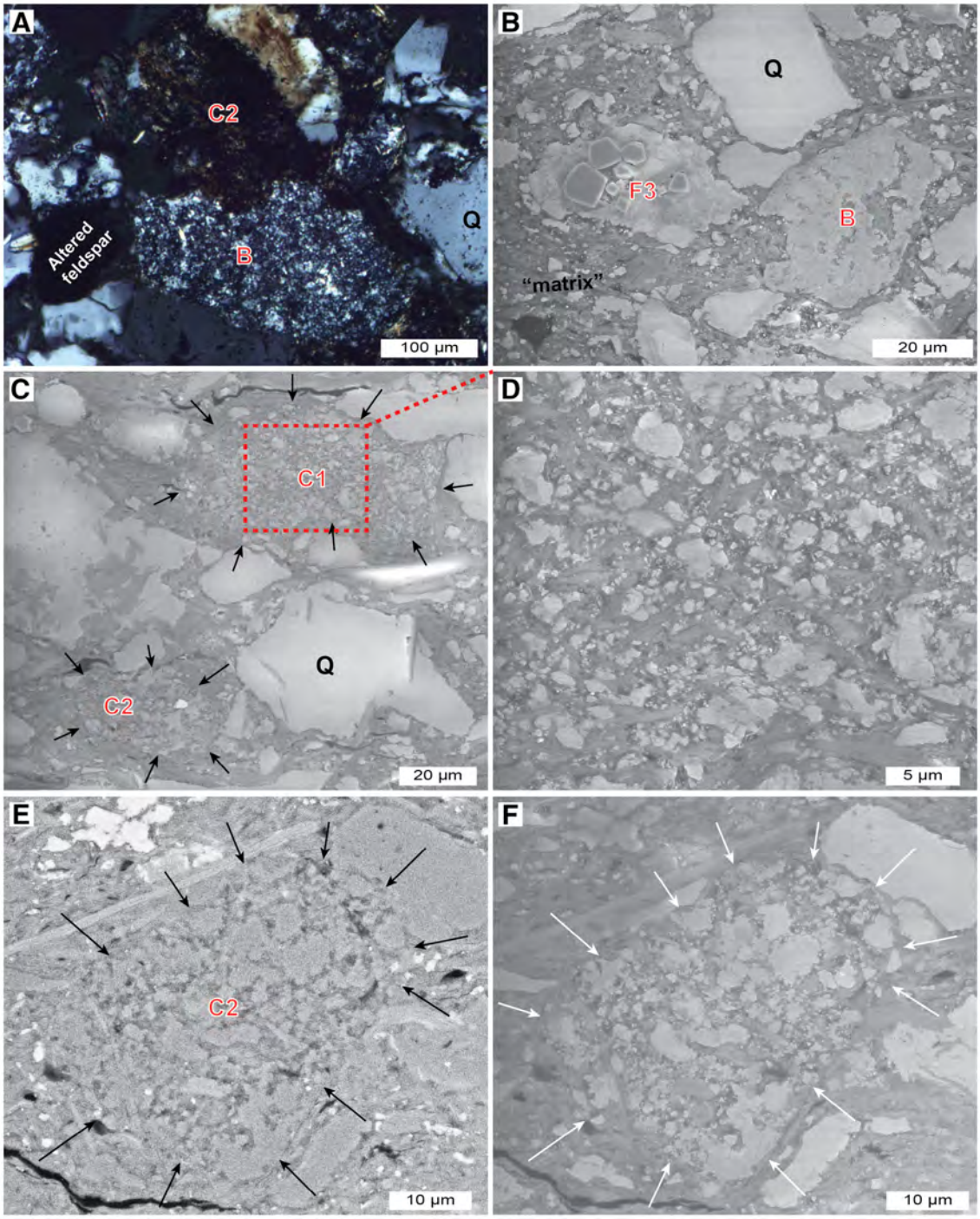

Fig. 4. Petrographic characteristics of sedimentary rock fragments. Red letters indicate different types of mud-dominated composite particles (MCPs) as listed in Table 1. (A) Photomicrograph shows a type B MCP (chert fragment) characterized by 'salt and pepper' texture in an incised valley sandstone sample. (B) Type B MCP (chert fragment) and a type F3 MCP (benthic-foraminifera-like rip-up clast) in a prodelta mudstone sample. (C) Type C1 MCP (clay-mineral-rich shale lithic) and a type C2 MCP (quartz-rich shale lithic) in a prodelta mudstone sample. Note both shale lithics are resistant to compaction and act as framework grains. (D) Closer view of the type C1 MCP (clay-mineral-rich shale lithic) in (C). (E) and (F) Closer view of a type C2 MCP (quartz-rich shale lithic) in a prodelta mudstone sample. (A) was acquired in cross-polarized light. (B) to (D) and (F) are secondary electron images. Black and white arrows in (C), (E) and (F) indicate the outlines of MCPs. (E) was taken in backscatter electron mode. Q, quartz.

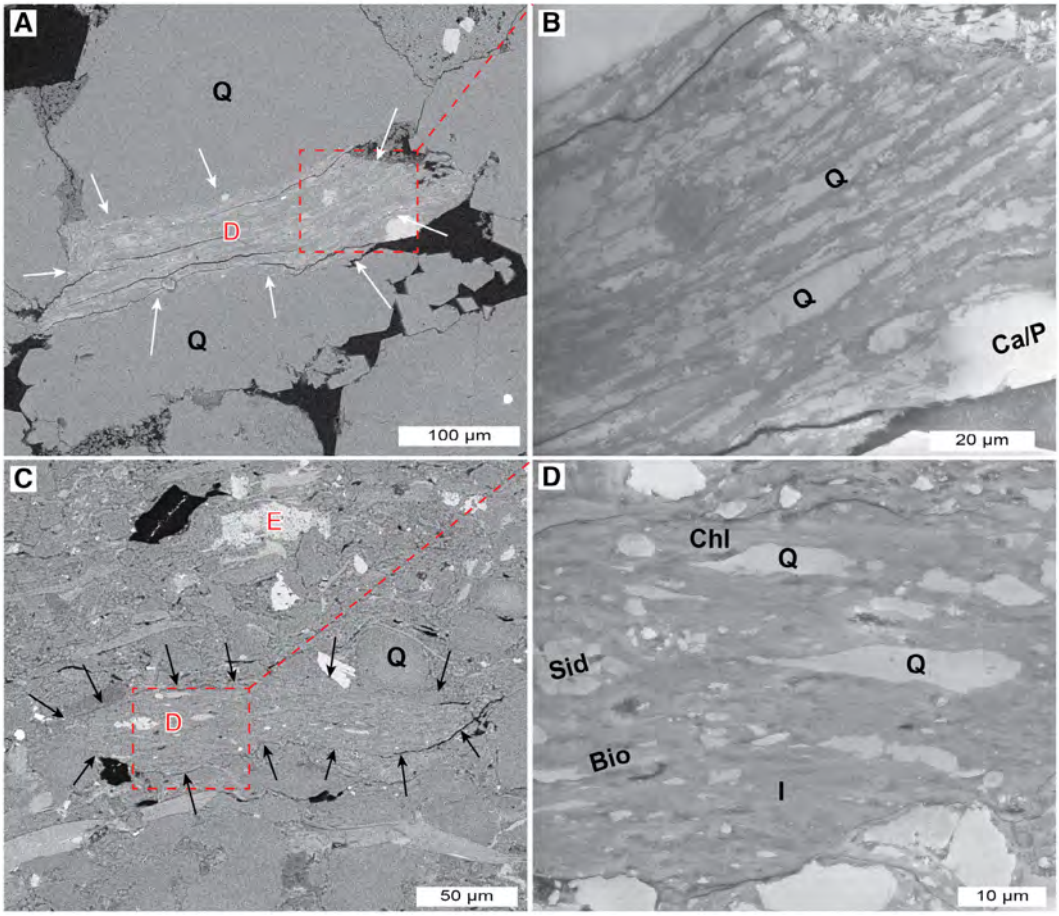

Fig. 5. Scanning electron microscopy (SEM) photomicrographs showing petrographic characteristics of type D mud-dominated composite particle (MCP) (metamorphic rock fragment). (A) From an incised valley sandstone sample. (B) Closer view of the metamorphic rock fragment shown in (A). (C) From a prodelta mudstone sample. (D) Closer view of the metamorphic rock fragment in (C). Note the elongated quartz crystals in both metamorphic rock fragments shown in (B) and (D). (A) and (C) are backscatter images. (B) and (D) are secondary electron images. Arrows in (A) and (C) indicate the outlines of MCPs. Q, quartz; Ca/P, apatite; E (red letter), chlorite/siderite clast; Chl, chlorite; Sid, siderite; Bio, biotite; I: illite.

chlorite/siderite-rich rocks associated with the Precambrian iron formations exposed in the catchment area (James, 1951; Bekker *et al.*, 2010).

Type F MCPs (rip-up clasts) can be recognized based on evidence indicating reworking/erosion of previously deposited surficial or shallowing buried muds. Argillaceous rip-up clasts (Type F1) usually show indentation by surrounding harder particles or a significant degree of vertical shortening (Fig. 7A to D) and are interpreted as derived from erosion of previously deposited muds that were still water-rich but had become cohesive enough to resist disaggregation (Schieber *et al.*, 2010). The early diagenetic siderite cement (Mozley, 1989; Bhattacharya & Walker, 1991a) in the sideritic rip-up clasts (Type F2) also indicates reworking/erosion of previously buried muds (Fig. 7A and E). The presence of siliceous (benthic-foraminifera-like) rip-up clasts (Type F3) provides another line of evidence of reworking/erosion of the seabed, during which surficial or shallowly buried muds containing benthic agglutinated foraminifera were eroded and broken into siliceous rip-up clasts (Fig. 8). Due to better cementation, sideritic and siliceous rip-up clasts are more resistant to compaction compared to argillaceous rip-up clasts. In sandstone beds, mud rip-up clasts are more easily recognized (Fig. 7A and B). When surrounded by the fine-grained matrix, the limited lithological contrast may

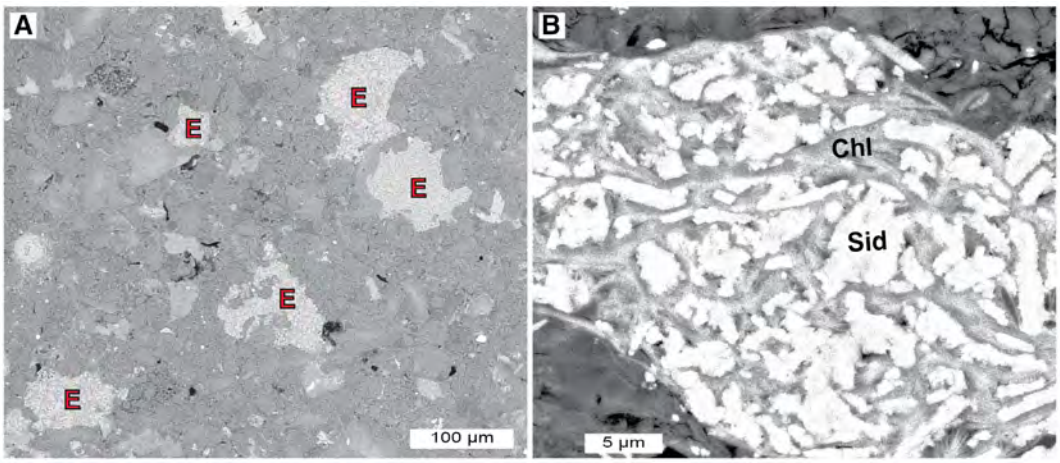

Fig. 6. Scanning electron microscopy (SEM) photomicrographs (backscatter images) showing petrographic characteristics of type E mud-dominated composite particle (MCP) (chlorite/siderite clast). (A) Image from an incised valley sandstone sample. (B) Closer view of a chlorite/siderite clast in a prodelta mudstone sample. Chl, chlorite; Sid, siderite.

preclude the recognition of argillaceous rip-up clasts, especially faecal pellets or burrows, sometimes may also show a similarly lenticular fabric (Fig. 7C). Nevertheless, the lens-shaped particles in Fig. 7C (indicated by orange arrows) were identified as argillaceous rip-up clasts rather than faecal pellets or burrows based on several additional criteria. Firstly, these particles occur directly above an erosional surface (dashed line in Fig. 7C). The erosion of the muddy substrate would likely produce some mud rip-up clasts. Secondly, the sedimentation rate following the erosional event was probably too high to allow any benthic organisms to colonize the deposits. If these particles were reworked planktonic faecal pellets, they would contain some plankton debris, which is not the case. Rather, the close similarity between the rip-up clasts and the muddy substrate in both composition and texture (Fig. 7D) strongly suggest a direct link. Detailed SEM analysis, integrated with the depositional context inferred from careful analysis of small-scale sedimentary structures, can aid in distinguishing argillaceous rip-up clasts from faecal pellets or burrows.

Another important type of MCPs presumably present in the Dunvegan delta system is floccules (Type G MCP), which are also water-rich (85% or more original water content by volume) MCPs consisting dominantly of clay-sized to fine-silt sized mineral grains and organic debris (Schieber *et al.*, 2010). Because floccules have essentially the same composition as the fine-grained matrix (for example, the matrix in Fig. 7D), it is rather challenging to justify the original presence of individual floccules by directly recognizing their outlines in mudstones after compaction even through SEM analysis (Shchepetkina *et al.*, 2018). Nevertheless, the presence of traction-generated structures such as erosional base, starved silt ripples (black arrows in Fig. 7C) and parallel laminations in some mudstone intervals (for example, the muddy substrate in Fig. 7C) indicate that these apparently fine-grained mudstones were likely deposited from bedload transport of mud floccules (Schieber *et al.*, 2007).

Variations in the composition and apparent grain size from proximal to distal deposits

All MCP types except for floccules are present from the proximal incised valley to distal prodelta environments. In addition to single mineral grains and recognizable MCPs (i.e. all types of MCPs except for floccules), prodelta mudstones (Fig. 9I and J), compared to their proximal counterparts (Fig. 9A, B, D and E), contain a distinctly higher proportion of fine-grained matrix in which no distinct MCPs can be identified (Fig. 9I and J). The fine-grained matrix consists dominantly of clay-sized to fine-silt-sized grains and has a relatively uniform texture (for example, Figs 3A, 4B and 7D), similar to some argillaceous mud rip-up clasts (Fig. 7D) and presumably floccules.

Both monocrystalline quartz and recognizable MCPs noticeably decrease in size from proximal to distal settings (Fig. 9). Both incised

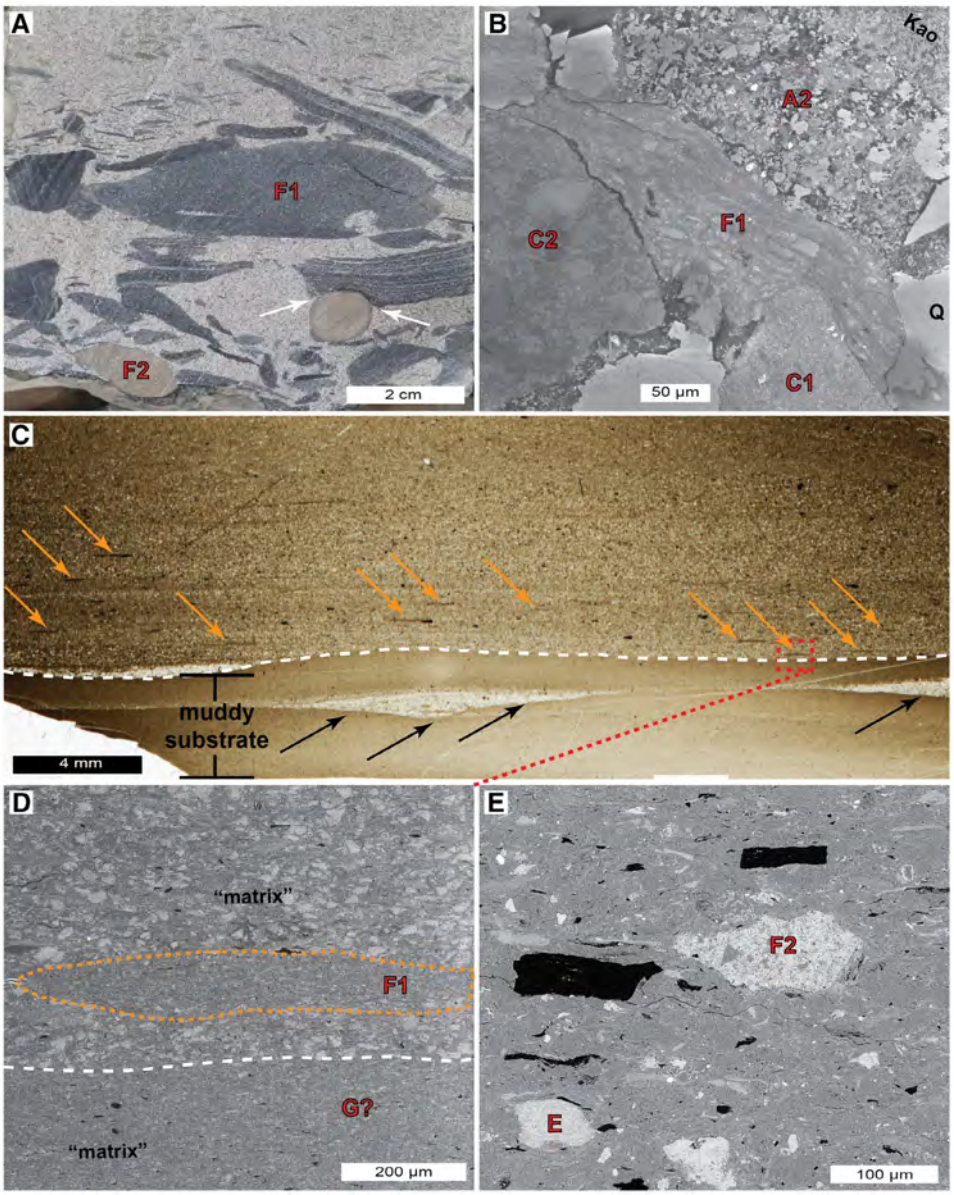

Fig. 7. Characteristics of type F1 mud-dominated composite particle (MCP) (argillaceous rip-up clast) and type F2 MCP (sideritic rip-up clast). (A) Core photograph showing common mud rip-up clasts in an incised valley sandstone sample. Brown rip-up clasts are cemented by siderite and more resistant to compaction, whereas dark-coloured ones are argillaceous in composition and 'flattened' to various degrees. Note that one relatively soft argillaceous rip-up clast is indented by a harder sideritic rip-up clast (white arrows). Also note the wide range of grain size of argillaceous rip-up clasts. (B) Scanning electron microscopy (SEM) photomicrograph showing a highly 'flattened' and indented argillaceous rip-up clast in an incised valley sandstone sample. (C) Scanned thin section image of a prodelta 'mudstone'. The presence of common argillaceous rip-up clasts (orange arrows) right above an erosional surface (white dashed line) indicates that the rip-up clasts were probably derived from erosion of the muddy substrate. The muddy substrate shows traction-generated structures including erosional base and starved silt ripples (black arrows). (D) Closer view of the dashed area in (C) showing characteristics of the muddy substrate below the erosional surface (white dashed line) and an argillaceous rip-up clast (outlined in orange). The presence of traction-generated structures [black arrows in (C)] indicates that the apparently fine-grained interval below the erosional surface was likely deposited from bedload transport of mud floccules (indicated by the red letter 'G'), although their original outlines cannot be recognized. (E) SEM photomicrograph (backscatter image) showing a type F2 mud-dominated composite particle (MCP) (sideritic rip-up clast) and a type E MCP (chlorite/siderite) clast in a prodelta mudstone sample. (B) and (D) are secondary electron images.

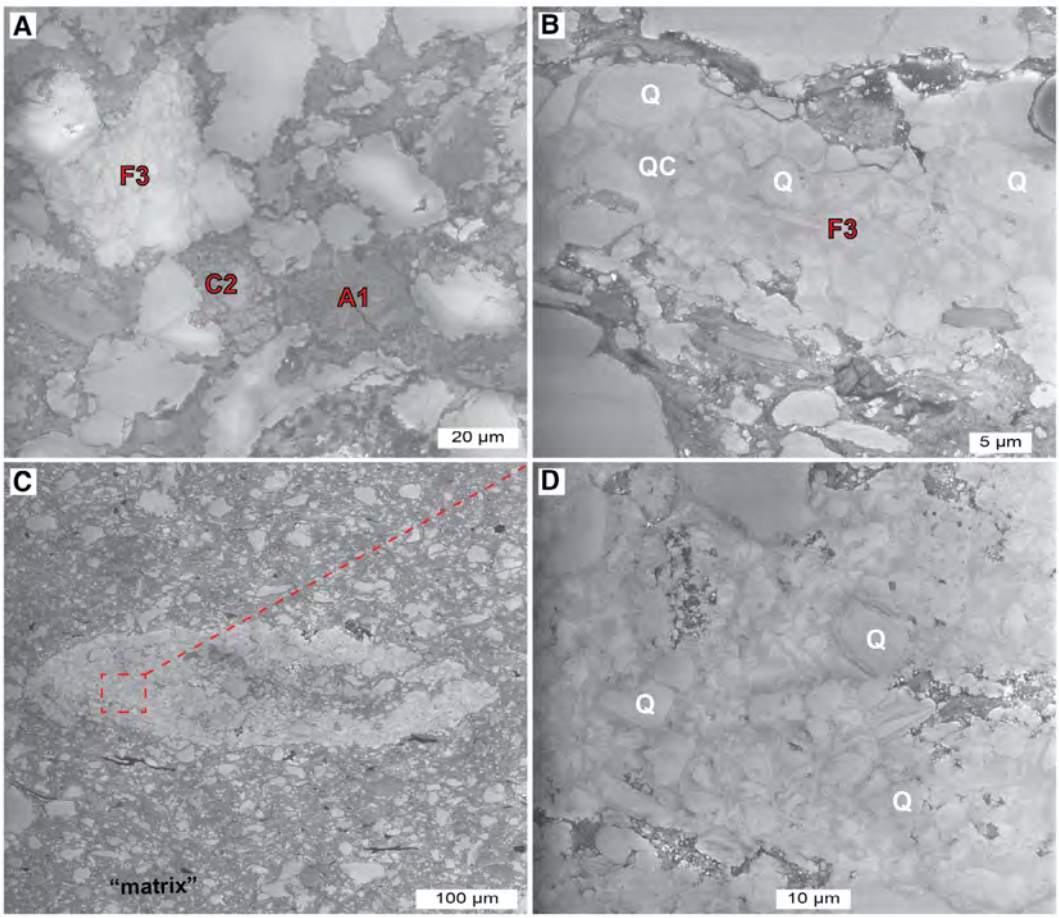

Fig. 8. (A) and (B) Scanning electron microscopy (SEM) photomicrograph showing petrographic characteristics of type F3 mud-dominated composite particles (MCPs) (siliceous rip-up clasts). (C) A complete collapsed benthic agglutinated foraminifera. The aggregates of silt-sized particles probably represent the 'detrital cover' that agglutinated foraminifera erected around themselves while building a new chamber (Pike & Kemp, 1996). (D) Closer view of the area within the agglutinated foraminifera shown in (C). The similarity between the texture of the agglutinated foraminifera in (D) and those type F3 MCPs (siliceous rip-up clasts) shown in (A) and (B) indicates that siliceous rip-up clasts are broken pieces of benthic agglutinated foraminifera. Q, quartz; QC, quartz cement. All images are secondary electron images and from prodelta mudstone samples.

Fig. 9. Representative scanning electron microscopy (SEM) images and grain size (circle equivalent diameter) distribution of monocrystalline quartz and mud-dominated composite particles (MCPs) from the incised valley (A) to (C), proximal delta front (D) to (F), distal delta front (G) and (H), to prodelta (I) to (K) facies associations (samples 'a' to 'd' in Fig. 2). The MCPs account for approximately 32%, 31%, 14% and 20% (volume by 2D area) in (A), (D), (G) and (I), respectively. Note the x axis (particle size) in (C), (F), (H) and (K) is logarithmic in millimetres. Tick marks on the y axes indicate different types of particles, which are coded by different colours. Note that (A), (B), (D) and (E) contain no fine-grained matrix [the 'dirty' areas in (A) and (D) can be readily recognized as various types of MCPs that have different fine-grained textures] in (B) and (E), whereas (G), (I) and (J) contain a higher proportion (>20%) of fine-grained matrix ('dirty' areas) in which no distinct type of MCP can be confidently identified. SEM images for each depositional environment are from only one representative view, whereas the plots of grain-size distribution are based on results from SEM images from four to five representative views of each depositional environment. (A), (D), (G) and (I) are secondary electron SEM images. (B), (E) and (J) are backscattered SEM images. Q, quartz; cc, calcite cement.

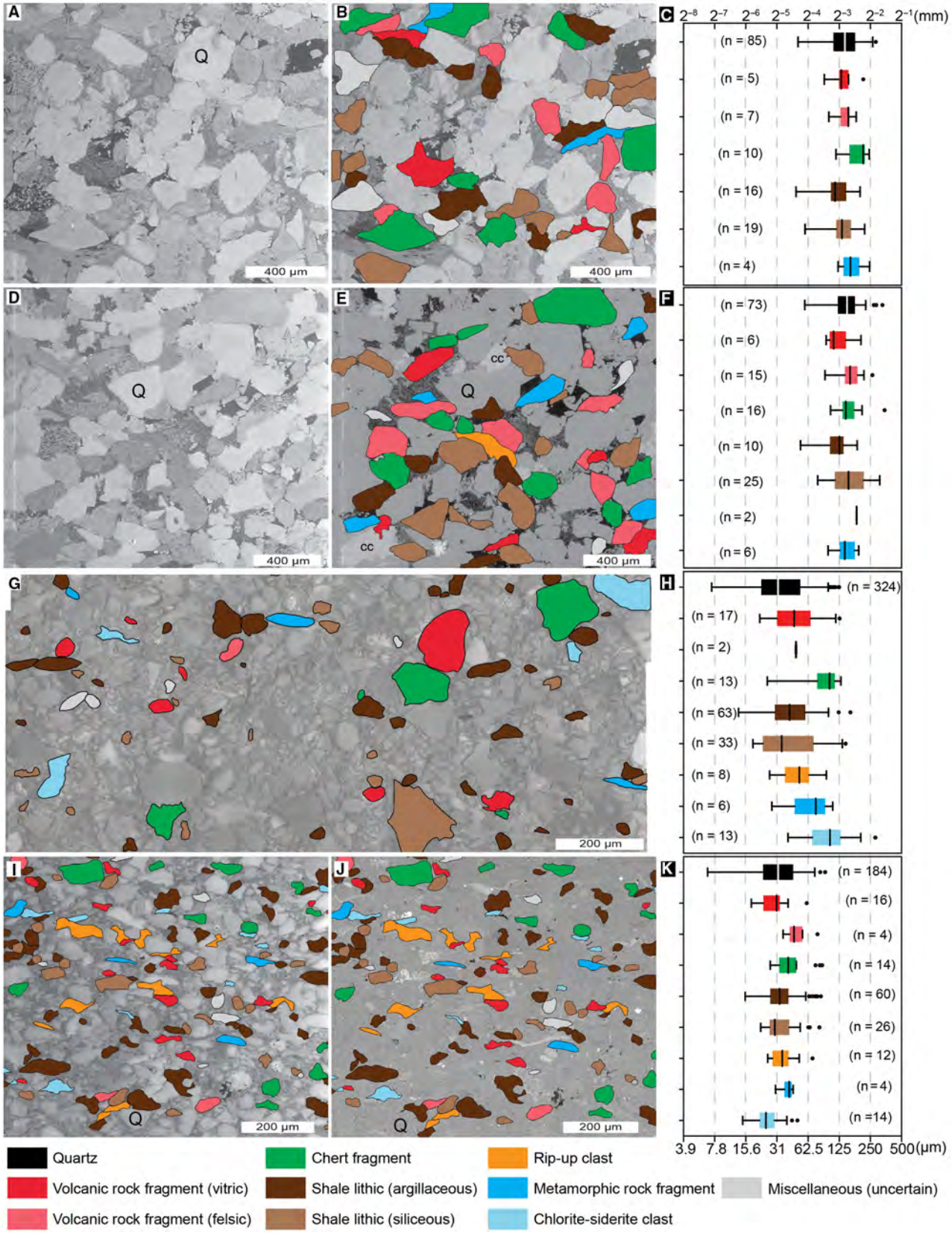

valley and proximal delta front facies contain dominantly fine-sand-sized (125 to 250 μm) quartz grains and a very similar suite of MCP types (Fig. 9C and F). In distal delta front and prodelta deposits most quartz grains are in the medium to coarse silt range, while the 'largest' quartz grains are of smaller (finer) size in prodelta deposits (Fig. 9H and K). Similarly, all recognized MCPs in the prodelta facies are overall finer in size when compared to those in the distal delta front facies (Fig. 9G and K).

DISCUSSION

Allochthonous and autochthonous mud-dominated composite particles

Because the incised valley trunk channel was located between the final confluence of the tributary network and the initial bifurcation of the distributary system (Fig. 1), it can be considered as a local depocentre of sediments eroded from the entire catchment area. The fact that samples from incised valley to prodelta facies show a similar suite of MCPs (Fig. 9) indicates that a large portion of MCPs deposited in offshore marine environments were derived from the hinterland via rivers and are allochthonous in nature. In this respect, allochthonous MCPs within offshore deposits are lithic fragments that were durable enough to survive transport and reworking in river and marine environments (Schieber, 2016). The diverse types of lithic fragments (Figs 3) to 6) indicate that sediments of the Dunvegan Formation were derived from erosion of basement exposures as well as recycling of older sedimentary rocks exposed within the Sevier orogenic belt, consistent with detrital zircon provenance data from sandstones in the Dunvegan Formation (Buechmann, 2013; Quinn *et al.*, 2016).

Mud rip-up clasts in the Dunvegan depositional system are autochthonous MCPs derived from intra-basinal erosion. The erosion of portions of allomember E2 (highstand prodelta mudstones) at the sequence boundary below the incised valley system of allomember E1 (Fig. 2) likely generated abundant mud rip-up clasts that were then dispersed across the entire Dunvegan lowstand system (Figs 2 and 7A). In addition to these deep incision (metre-scale) events associated with rapid relative fall of sea level, mud rip-up clasts were probably also produced when intermittent reworking and erosion of surficial or shallowly buried muds occurred in the Dunvegan delta system as a consequence of common fluvial-dominated and storm-dominated processes (for example, surge-type turbidity current, hyperpycnal flow and storm surge; Bhattacharya & MacEachern, 2009). Unlike siliceous or sideritic rip-up clasts, which were cemented during early diagenesis, newly formed argillaceous rip-up clasts would have had varying water content in accordance with the depth from which they were eroded. After final deposition and compaction, rip-up clasts with variable water content can be expected to be deformed and 'flattened' to various degrees and show highly variable aspect ratios (Fig. 7).

Floccules are also considered here as autochthonous MCPs because they were likely formed in the ocean basin, despite that the dominant constituents of floccules (i.e. clay-sized to fine-silt-sized grains) were originally derived from hinterland weathering. Studies of modern shelves suggest that upon entering the sea, fine-grained sediments supplied by rivers should have undergone rapid aggregation in the highly turbid waters at the river mouths (Sternberg *et al.*, 1999; Hill *et al.*, 2000). The packaging of fine-grained (clay-sized to fine-silt-sized) sediments into floccules could increase the effective settling velocity of their clay-sized to silt-sized constituent grains by one to two orders of magnitude, and result in the rapid settling of fine-grained sediments close to the river mouth (Sternberg *et al.*, 1999; Hill *et al.*, 2000; McCool & Parsons, 2004). The subsequent transport and deposition of floccules was then likely subject to currents and waves/storm actions in the bottom boundary layer (Hill *et al.*, 2001). Although it is almost impossible to detect the outlines of individual floccules in mudstones after compaction, the common presence of bedload structures (Figs 2 and 7C) in Dunvegan prodelta mudstones suggests that their fine-grained matrix was probably transported and deposited as floccules (Schieber *et al.*, 2007).

Actual (depositional) grain size of mudstones

Although the Dunvegan prodelta deposits were described as mudstones based on their fine-grained appearance in cores (containing dominantly clay-sized to silt-sized mineral grains that cannot be resolved with a hand lens), SEM analysis shows them to contain a significant proportion of coarse silt to fine-sand-sized MCPs (Fig. 9). Regardless of origin or type, allochthonous MCPs decrease in average grain size from

incised valley (fine sand; Fig. 9) to prodelta (coarse silt; Fig. 9), due to preferential deposition of coarser particles in proximal settings. Although distal prodelta mudstones are characterized by a paucity of easily recognizable MCPs, studies of modern shelf muds (Sternberg *et al.*, 1999; Hill *et al.*, 2000) make it seem plausible that they consisted largely of autochthonous MCPs such as water-rich mud rip-up clasts and floccules. These water-rich MCPs can be up to several hundreds of micrometres (medium-sand to coarse-sand size) in length (Fig. 7C and D; Sternberg *et al.*, 1999) and are transport-equivalent to quartz silt/sand (based on the concurrence of these particles in these deposits; Fig. 7A and B). Due to their water-rich nature these relatively soft argillaceous rip-up clasts and floccules may disaggregate during energetic floods or storms due to high turbulence-induced stress or collision with harder particles (Hill *et al.*, 2001). The observation of multiple types of mud rip-up clasts (Figs 7 and 8) indicates that depositional events strong enough to rework/erode the muddy seabed were not uncommon. Therefore, it is likely that muds in the Dunvegan delta system underwent multiple cycles of deposition and resuspension before arriving at their final site of deposition. During each cycle of reworking and advection, finer-grained single mineral grains and allochthonous MCPs, newly formed rip-up clasts, as well as fine-grained sediments derived from disaggregated argillaceous rip-up clasts and floccules, will be preferentially transported and deposited in more distal settings. These disaggregated fine-grained sediments, however, would most likely re-flocculate when turbulence-induced stress decreased (Hill *et al.*, 2001). Thus, the distal Dunvegan mud deposits would be dominated by argillaceous rip-up clasts and floccules.

Because of their original water-rich nature and minimal lithological contrast, the recognition of autochthonous MCPs in the rock record is greatly facilitated when they are surrounded by grains/particles with sufficient compositional or textural contrast (Figs 7B and 10). Outside of such fortuitous instances, outlines of original water-rich MCPs in ancient mudstones are no longer discernible and they merge into what is commonly referred to as 'fine-grained matrix' (Figs 7D, 9I, 9J, 10E and 10F; Laycock *et al.*, 2017; Li & Schieber, 2018; Shchepetkina *et al.*, 2018). Therefore, the apparent decrease in grain size and increase in the proportion of 'fine-grained matrix' from the proximal to distal marine environments does not necessarily reflect a decrease in the actual grain size of the transported particles, but rather a decrease in the amount of more easily recognized allochthonous MCPs, and a concomitant increase in autochthonous MCPs with low textural preservation potential (Fig. 10).

One should also note that the supposed fine-grained nature of mudstones (or the designation of rocks as mudstones) is in most instances predicated on the observed grain size of mineral constituents rather than the grain size of underlying composite particles determined through high end petrographic studies (as in this study). This *a priori* assumption of fine grain size is at the root of the common overemphasis of the role of suspension settling in the accumulation of many ancient mudstone successions. Given that the settling velocity of disaggregated fine-grained sediments is one to two orders of magnitude lower than that of floccules (or rip-up clasts) (Sternberg *et al.*, 1999), and considering the high sedimentation rates of the Dunvegan system (1 to 10 m ka^{-1}; Bhattacharya *et al.*, 2019), the deposition of prodelta mudstones in the energetic Dunvegan system would have been physically impossible without MCPs dominating transport and depositional processes.

A comprehensive understanding of the actual (depositional) grain size of mudstones is therefore critical to accurately interpret the depositional processes and environments of these rocks. The identification of different types of allochthonous MCPs requires SEM analysis of highly polished mudstone samples (ultra-thin thin sections and preferably ion-milled samples). Despite the low preservation potential of autochthonous MCPs in fully compacted mudstones, careful SEM analysis, integrated with detailed analysis of small-scale sedimentary features (for example, bedload structures), can inform on the presence and abundance of water-rich MCPs, as well as the actual (depositional) grain-size of mudstones.

Along the depositional profile examined in this study, autochthonous MCPs become increasingly dominant components in relatively distal prodelta settings, whereas mudstones deposited in proximal settings contain a higher proportion of readily recognized allochthonous MCPs. The ratio between the amounts of allochthonous and autochthonous MCPs in marine mudstones, carefully inferred from integrated petrographic and sedimentological analysis, may therefore serve as a useful indicator of their depositional setting (proximal versus distal; Fig. 10) and can be

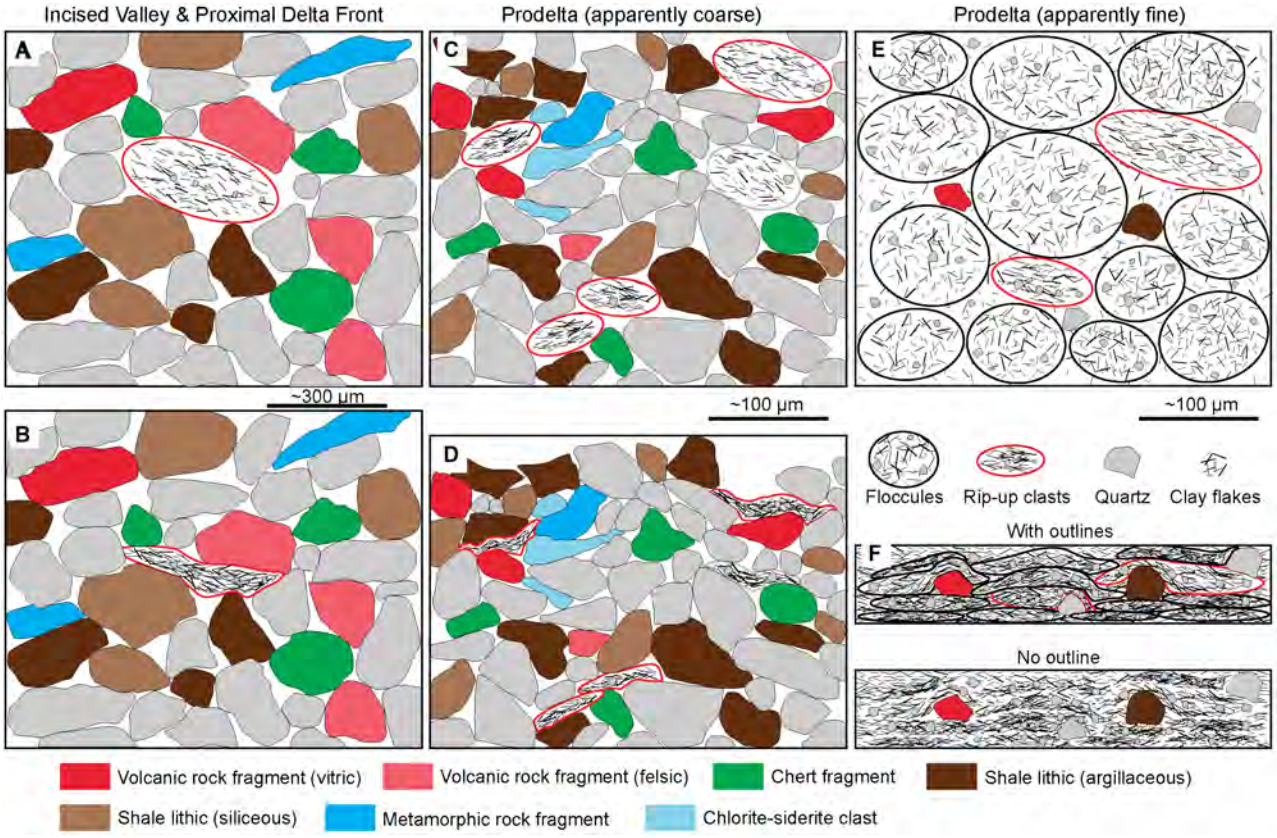

Fig. 10. Schematic drawing illustrating differences in the preservation potential water-rich autochthonous mud-dominated composite particles (MCPs) (mud rip-up clasts and floccules) from proximal and distal marine environments. (A) and (B) Incised valley and proximal delta front environments. (C) and (D) Prodelta (proximal) environment. (E) and (F) Prodelta (distal) environment. Upper row: before compaction. Lower row: after compaction (only mechanical compaction is considered). Rip-up clasts depicted in these drawings are exclusively argillaceous in composition. Rip-up clasts that are well cemented during early diagenesis (for example, siliceous and sideritic in composition) would behave similarly to relatively 'hard' allochthonous MCPs during transport, deposition and compaction. In relatively proximal settings, sediment supply of allochthonous MCPs is high. Additionally, collision between autochthonous water-rich MCPs and hard particles (for example, quartz, feldspar and hard MCPs) can result in disaggregation of these water-rich MCPs. Consequently, few autochthonous MCPs are generally preserved in proximal deposits, and the preserved autochthonous MCPs are relatively easy to be identified based on distinct compositional and textural characteristics [(A) to (D)]. In distal prodelta settings, autochthonous MCPs increase in abundance in seabed sediments. Higher abundance of water-rich MCPs at deposition results in higher degree of compaction. Despite their abundance, it is very challenging to recognize outlines of individual mud rip-up clasts and floccules after compaction due to their close compositional similarity and water-rich nature [(E) and (F)]. It is important to note that outlines of floccules and mud rip-up clasts indicated in (E) and (F) are only for illustrative purposes. Considering the close compositional and textural similarity, these water-rich MCPs, even before compaction (E), are not easy to differentiate from one another – imagine how challenging it would be to identify individual MCPs without outlines in (E).

applied to stratigraphic analysis (for example, sequence stratigraphy) of mudstone-dominated successions characterized by obscure variations in apparent grain size.

Complex provenance and polycyclic origin of mudstones

Results of this study indicate that allochthonous MCPs (i.e. lithic fragments), derived from the hinterland via rivers, constitute an important component of offshore marine mudstones. Although sand-sized allochthonous MCPs may be preferentially deposited in proximal settings close to the river mouth (Fig. 9), allochthonous MCPs ranging from medium silt to very fine sand size can be dispersed to more distal settings and have been documented in outer shelf (*ca* 100 km away from the palaeoshoreline) deposits of the Tununk Shale Member of the Mancos Shale (south-central Utah,

USA; Li & Schieber, 2018). The types of allochthonous MCPs documented in the Dunvegan prodelta mudstones are likely not exhaustive because any lithic fragments with fine-grained internal texture may end up as allochthonous MCPs in marine mudstones. The analysis of MCPs can therefore aid in unravelling potentially complex provenance and polycyclic origins of marine mudstones, a critical yet largely neglected issue in the use of mudstone successions as archives of climate and environmental change.

Due to the apparent fine-grained nature and homogeneity of mudstones, researchers typically resort to analysis of more readily acquired proxy data such as mineralogical, elemental and isotopic composition to infer the conditions under which mudstones were deposited. However, the wide range of lithic fragments and recycled detritus documented in Dunvegan prodelta 'mudstones' and other successions studied in a similar fashion (Li & Schieber, 2018) indicate that compositional signals thought to be characteristic of climatic and environmental conditions can be (and likely are) mixed or overprinted by variants of these signals associated with MCPs that formed under different environmental conditions and ages. The roles of MCPs in the formation of mudstone successions need to be critically investigated, because they provide valuable information regarding the provenance and dispersal pathways of these rocks. It is also critical to examine in detail how various types and amounts of MCPs in mudstones may modify or overprint mineralogical and elemental signals characteristic of climate and environmental conditions, so as to enable accurate interpretations of palaeoclimate and environmental conditions based on proxy data from mudstone successions.

CONCLUSIONS

1 Marine mudstones can contain diverse types of mud-dominated composite particles (MCPs) derived from both allochthonous and autochthonous sources. Dunvegan prodelta 'mudstones', as well as many other marine mudstones, are probably only fine-grained in terms of their mineralogical composition.

2 The common presence of coarse silt to sand-sized MCPs in marine mudstones reinforces the important role of bedload transport of mud under relatively energetic conditions. Detailed petrographic analysis of the actual depositional grain size and components, integrated with careful detailed analysis of sedimentary structures, is critical to accurate interpretation of mudstone depositional processes and environments.

3 The mixing of various types of MCPs with different compositions and textures essentially produced the compositional and textural heterogeneity seen in petrographic thin sections of Dunvegan mudstones, a result that likely applies to many other mudstone successions elsewhere.

4 The analysis of mud-dominated composite particles in of mudstones can inform about their potentially complex provenance and transport history (for example, polycyclic), and can provide indispensable insights for effective extraction of palaeoenvironmental information preserved in the mudstone record.

ACKNOWLEDGEMENTS

We are grateful for the constructive review and editorial comments of Drs Korhan Ayranci, Janok Bhattacharya, Joao Trabucho Alexandre, Chris Fielding and Peir Pufahl. This research was supported by the sponsors of the Indiana University Shale Research Consortium. We acknowledge geoLOGIC for access to their well database geoSCOUT, and Alberta Energy Regulator for access to sampling of cores.

DECLARATION OF INTEREST STATEMENT

We declare that we do not have any commercial or associative interest that represents a conflict of interest in connection with the work submitted.

DATA AVAILABILITY STATEMENT

The data that support the findings of this study are available from the corresponding author upon reasonable request.

REFERENCES

Bekker, A., **Slack, J.F.**, **Planavsky, N.**, **Krapež, B.**, **Hofmann, A.**, **Konhauser, K.O.** and **Rouxel, O.J.** (2010) Iron formation: the sedimentary product of a complex interplay among mantle, tectonic, oceanic, and biospheric processes. *Econ. Geol.*, **105**, 467–508.

Bhattacharya, J. and **Walker, R.G.** (1991a) River- and wave-dominated depositional systems of the Upper Cretaceous Dunvegan Formation, northwestern Alberta. *Bull. Can. Petrol. Geo.*, **39**, 165–191.

Bhattacharya, J. and **Walker, R.G.** (1991b) Allostratigraphic subdivision of the Upper Cretaceous Dunvegan, Shaftesbury, and Kaskapau formations in the northwestern Alberta subsurface. *Bull. Can. Petrol. Geol.*, **39**, 145–164.

Bhattacharya, J.P. and **MacEachern, J.A.** (2009) Hyperpycnal rivers and prodeltaic shelves in the Cretaceous seaway of North America. *J. Sed. Res.*, **79**, 184–209.

Bhattacharya, J.P., **Miall, A.D.**, **Ferron, C.**, **Gabriel, J.**, **Randazzo, N.**, **Kynaston, D.**, **Jicha, B.R.** and **Singer, B.S.** (2019) Time-stratigraphy in point sourced river deltas: application to sediment budgets, shelf construction, and paleo-storm records. *Earth Sci. Rev.*, **199**, 102985.

Buechmann, D.L. (2013) *Provenance, Detrital Zircon U-Pb Geochronology and Tectonic Significance of Middle Cretaceous Sandstones from the Alberta Foreland Basin*. University of Houston, Houston, Texas, 97 pp.

Hill, P.S., **Milligan, T.G.** and **Geyer, W.R.** (2000) Controls on effective settling velocity of suspended sediment in the Eel River flood plume. *Cont. Shelf Res.*, **20**, 2095–2111.

Hill, P.S., **Voulgaris, G.** and **Trowbridge, J.H.** (2001) Controls on floc size in a continental shelf bottom boundary layer. *J. Geophys. Res. Oceans*, **106**, 9543–9549.

James, H.L. (1951) Iron formation and associated rocks in the Iron River district, Michigan. *GSA Bull.*, **62**, 251–266.

Kauffman, E.G. (1985) Cretaceous evolution of the Western Interior Basin of the United States. *SEPM Guidebook*, **4**, iv–xiii.

Laycock, D.P., **Pedersen, P.K.**, **Montgomery, B.C.** and **Spencer, R.J.** (2017) Identification, characterization, and statistical analysis of mudstone aggregate clasts, Cretaceous Carlile Formation, Central Alberta, Canada. *Mar. Petrol. Geol.*, **84**, 49–63.

Lazar, O.R., **Bohacs, K.M.**, **Macquaker, J.H.S.**, **Schieber, J.** and **Demko, T.M.** (2015) Capturing key attributes of fine-grained sedimentary rocks in outcrops, cores, and thin sections: nomenclature and description guidelines. *J. Sed. Res.*, **85**, 230–246.

Li, Z. and **Schieber, J.** (2018) Composite particles in mudstones: examples from the late Cretaceous Tununk Shale Member of the Mancos Shale Formation. *J. Sed. Res.*, **88**, 1319–1344.

Li, Z., **Schieber, J.** and **Bish, D.** (2020) Decoding the origins and sources of clay minerals in the Upper Cretaceous Tununk Shale of south-central Utah: implications for the pursuit of climate and burial histories. *Deposit. Rec.*, **6**, 172–191.

Macquaker, J.H.S. and **Bohacs, K.M.** (2007) On the accumulation of mud. *Science*, **318**, 1734.

McCool, W.W. and **Parsons, J.D.** (2004) Sedimentation from buoyant fine-grained suspensions. *Cont. Shelf Res.*, **24**, 1129–1142.

Mozley, P.S. (1989) Relation between depositional environment and the elemental composition of early diagenetic siderite. *Geology*, **17**, 704–706.

Nadeau, P.H. and **Reynolds, R.C.** (1981) Volcanic components in pelitic sediments. *Nature*, **294**, 72–74.

Pike, J. and **Kemp, A.E.S.** (1996) Silt aggregates in laminated marine sediment produced by agglutinated foraminifera. *J. Sed. Res.*, **66**, 625–631.

Plint, A.G. (2014) Mud dispersal across a Cretaceous prodelta: Storm-generated, wave-enhanced sediment gravity flows inferred from mudstone microtexture and microfacies. *Sedimentology*, **61**, 609–647.

Plint, A.G. and **Cheadle, B.A.** (2015) Reply to the Discussion by Schieber on "Mud dispersal across a Cretaceous prodelta: Storm-generated, wave-enhanced sediment gravity flows inferred from mudstone microtexture and microfacies" by Plint (2014), *Sedimentology*, **61**, 609–647. 62, 394–400.

Plint, A.G. and **Wadsworth, J.A.** (2003) Sedimentology and palaeogeomorphology of four large valley systems incising delta plains, western Canada Foreland Basin: implications for mid-Cretaceous sea-level changes. *Sedimentology*, **50**, 1147–1186.

Potter, P.E., **Maynard, J.B.** and **Depetris, P.J.** (2005) *Mud and Mudstones: Introduction and Overview*. Springer-Verlag, Berlin Heidelberg, 297 pp.

Quinn, G.M., **Hubbard, S.M.**, **van Drecht, R.**, **Guest, B.**, **Matthews, W.A.** and **Hadlari, T.** (2016) Record of orogenic cyclicity in the Alberta foreland basin, Canadian Cordillera. *Lithosphere*, **8**, 317–332.

Sageman, B.B., **Murphy, A.E.**, **Werne, J.P.**, **Ver Straeten, C.A.**, **Hollander, D.J.** and **Lyons, T.W.** (2003) A tale of shales: the relative roles of production, decomposition, and dilution in the accumulation of organic-rich strata, Middle-Upper Devonian, Appalachian basin. *Chem. Geol.*, **195**, 229–273.

Schieber, J. (2015) Discussion: "Mud dispersal across a Cretaceous prodelta: Storm-generated, wave-enhanced sediment gravity flows inferred from mudstone microtexture and microfacies" by Plint (2014), Sedimentology 61, 609–647. *Sedimentology*, **62**, 389–393.

Schieber, J. (2016) Experimental testing of the transport-durability of shale lithics and its implications for interpreting the rock record. *Sed. Geol.*, **331**, 162–169.

Schieber, J., **Miclăuș, C.**, **Seserman, A.**, **Liu, B.** and **Teng, J.** (2019) When a mudstone was actually a "sand": Results of a sedimentological investigation of the bituminous marl formation (Oligocene), Eastern Carpathians of Romania. *Sed. Geol.*, **384**, 12–28.

Schieber, J., **Southard, J.** and **Thaisen, K.** (2007) Accretion of mudstone beds from migrating floccule ripples. *Science*, **318**, 1760–1763.

Schieber, J., **Southard, J.B.** and **Schimmelmann, A.** (2010) Lenticular shale fabrics resulting from intermittent erosion of water-rich muds—interpreting the rock record in the light of recent flume experiments. *J. Sed. Res.*, **80**, 119–128.

Shchepetkina, A., **Gingras, M.K.** and **Pemberton, S.G.** (2018) Modern observations of floccule ripples: Petitcodiac River estuary, New Brunswick, Canada. *Sedimentology*, **65**, 582–596.

Sternberg, R.W., **Berhane, I.** and **Ogston, A.S.** (1999) Measurement of size and settling velocity of suspended aggregates on the northern California continental shelf. *Mar. Geol.*, **154**, 43–53.

Manuscript received 8 June 2020; revision 4 September 2020; revision accepted 12 September 2020